# Adaptive Control of Brushless DC Motor Driven Robot Manipulators Using Legendre Polynomials

Irem Saka[1*], Sukru Unver[2], Erman Selim[3,4], Enver Tatlicioglu[3], and Erkan Zergeroglu[5]

***Abstract*— This paper presents a novel control strategy for brushless DC (BLDC) motor-driven, multi-degree-of-freedom robot manipulators, addressing the challenges posed by the highly nonlinear and coupled dynamics of the motor and manipulator. The proposed controller leverages the universal approximation property of Legendre polynomials, a class of orthogonal functions, to effectively compensate for modeling uncertainties and system nonlinearities. A rigorous stability analysis is conducted using Lyapunov-based methods, guaranteeing semi-global uniform ultimate boundedness of the closed-loop system. Experimental studies on an in-house developed BLDC-driven robotic device validate the effectiveness of the proposed controller, demonstrating its capability to achieve precise trajectory tracking with robust performance.**

## I. Introduction

The control of robot manipulators has been a central focus in robotics research due to its wide-ranging applications in industrial automation [1], medical robotics [2], and autonomous systems [3]. Among the various types of actuators used in robotic systems, brushless direct current (BLDC) motors have gained significant attention due to their high efficiency, compact design, and precise torque control capabilities [4], [5]. However, the integration of BLDC motors into multiple degrees of freedom (dof) robot manipulators introduces complex dynamics, including nonlinearities and coupling effects, which pose significant challenges for control design and stability analysis.

Traditional control strategies for robot manipulators often rely on simplified models that neglect the intricate dynamics of the actuators. In such approaches, controllers are typically designed at the torque level, disregarding the complexities of actuator behavior [6], [7], [8], [9]. While some studies do consider actuator dynamics, these approaches commonly rely on the assumption that joint torque varies linearly with the applied control signal, which may not accurately capture the true nonlinearities of the system [10], [11]. While these methods have demonstrated satisfactory performance in certain scenarios, they may fall short in achieving robust and precise control when the dynamics of the BLDC motor are coupled with the manipulator. This limitation underscores the need for advanced control techniques that explicitly account for the combined dynamics of the motor and the manipulator in both control design and stability analysis.

Various control strategies have been explored for robotic systems utilizing BLDC motors as joint actuators, including sliding mode control [12], proportional-integral-derivative control [13], high-frequency robust control [14], and adaptive control [15]. In recent years, orthogonal functions and polynomial-based approaches have gained prominence as powerful tools for control system design [16]. These methods leverage the mathematical properties of orthogonal functions, such as Legendre polynomials, to approximate complex nonlinear systems and derive control laws with guaranteed stability and performance [17]. The advantages of orthogonal functions include computational efficiency, ease of implementation, and robustness to system uncertainties [18]. Additionally, unlike traditional adaptive methods, they eliminate the need for regressor calculations, simplifying the control design. Notably, the work in [19] demonstrated the effectiveness of orthogonal functions in control design for robotic arms actuated by permanent magnet synchronous motors, providing a strong theoretical foundation for further research.

In this paper, we propose a novel control strategy for BLDC motor-driven multiple dof robot manipulators. Unlike most existing approaches, the proposed controller explicitly accounts for the coupled dynamics of the BLDC motor and the manipulator, providing a unified framework for control design and stability analysis. The key innovation lies in leveraging the orthogonal functions theorem and Legendre polynomials to derive a backstepping control law that successfully handles the interaction and nonlinear behavior inherent in the dynamic models of the mechanical and electrical components. A Lyapunov-based stability analysis guarantees that the closed-loop system remains semi-globally uniformly ultimately bounded with the proposed control strategy. The effectiveness of the proposed design is validated through experimental tests conducted on a custom-built two dof robotic arm.

The key contributions of this study can be summarized as follows:

- A control law is derived using Legendre polynomials, ensuring stability and robustness in the presence of both mechanical and electrical modeling uncertainties.
- A rigorous stability analysis is conducted using

[1]Irem Saka is with the Department of Mechanical Engineering, Ege University, Izmir, Turkiye. 91240000642@ogrenci.ege.edu.tr

[2]Sukru Unver is with the Department of Computer Engineering, Sivas University of Science and Technology, Sivas, Turkiye. sukru.unver@sivas.edu.tr

[3]Erman Selim and Enver Tatlicioglu are with the Department of Electrical & Electronics Engineering, Ege University, Izmir, Turkiye. erman.selim@ege.edu.tr, enver.tatlicioglu@ege.edu.tr

[4]Erman Selim is also with the Department of Mechanical & Mechatronics Engineering, University of Waterloo, Ontario, Canada. erman.selim@uwaterloo.ca

[5]Erkan Zergeroglu is with the Department of Computer Engineering, Gebze Technical University, Kocaeli, Turkiye. e.zerger@gtu.edu.tr

Lyapunov-based methods, demonstrating the semi-global uniform ultimate boundedness of the closed-loop system.
- The designed controller is validated through experimental studies, highlighting its effectiveness in achieving precise trajectory tracking. By exploiting the orthogonality property, the controller significantly enhances tracking accuracy.

The organization of the paper is outlined as follows. Section II introduces the system model and preliminaries. Section III is dedicated to the error system and control development, leveraging the universal approximation property of orthogonal basis functions. In Section IV, we perform a stability analysis based on Lyapunov techniques to guarantee uniform ultimate boundedness. Section V presents the experimental results that validate our theoretical findings, and Section VI finalizes the study by highlighting the main findings and suggesting future research.

## II. System Model and Preliminaries

The dynamic and electrical behavior of an $n$ dof robotic arm actuated by brushless DC motors is characterized by the following

$$M(q)\ddot{q} + V_m(q,\dot{q})\dot{q} + G(q) + F_d\dot{q} = \tau_d, \quad (1)$$

$$L_a\frac{dI_a}{dt} + RI_a + N_pL_bI_B\dot{q} + K_{T2}\dot{q} = V_a, \quad (2)$$

$$L_b\frac{dI_b}{dt} + RI_b - N_pL_aI_A\dot{q} = V_b, \quad (3)$$

where $q(t)$, $\dot{q}(t)$, $\ddot{q}(t) \in \mathbb{R}^n$ are the position, velocity, and acceleration vectors of the manipulator joints, respectively, $M(q) \in \mathbb{R}^{n\times n}$ represents the inertia matrix, $V_m(q,\dot{q}) \in \mathbb{R}^{n\times n}$ models centripetal and Coriolis effects, $G(q) \in \mathbb{R}^n$ demonstrates gravitational terms, $F_d \in \mathbb{R}^{n\times n}$ defines viscous friction matrix. The term $\tau_d(t) \in \mathbb{R}^n$ is expressed using the relation $\tau_d \triangleq (K_{T1}I_B + K_{T2})I_a$, with $K_{T1}$, $K_{T2} \in \mathbb{R}^{n\times n}$ denote torque transmission constants, $I_a(t)$, $I_b(t) \in \mathbb{R}^n$ are phase currents, with $I_A$, $I_B(t) \in \mathbb{R}^{n\times n}$ denoting their corresponding diagonal matrix representations. Armature inductances are given by $L_a$, $L_b \in \mathbb{R}^{n\times n}$, while $R \in \mathbb{R}^{n\times n}$ corresponds to the resistance matrices. $N_p \in \mathbb{R}^{n\times n}$ holds the values representing the count of pole pairs in the permanent magnet motors. Control inputs are provided through phase voltages $V_a(t)$, $V_b(t) \in \mathbb{R}^n$.

The dynamical terms in (1) satisfy the following standard properties that are fundamental to the analysis and controller design.

*Property 1:* The inertia matrix $M(q)$ possesses symmetry and positive definiteness, and adheres to the following set of inequalities [20]

$$w_1I_n \le M(q) \le w_2I_n, \quad (4)$$

where $w_1$, $w_2 \in \mathbb{R}$ denote positive constants. $I_n \in \mathbb{R}^{n\times n}$ defines the standard identity matrix.

*Property 2:* $M(q)$ and $V_m(q,\dot{q})$ exhibit a skew-symmetric relationship and satisfy the condition that [20]

$$z^T\left(\dot{M}(q) - 2V_m(q,\dot{q})\right)z = 0, \ \forall z \in \mathbb{R}^n. \quad (5)$$

## III. Error System and Control Development

This work proposes a control methodology aimed at enabling precise tracking of joint trajectories in robotic manipulators actuated by BLDC motors. Designing such a controller poses significant challenges due to the inherent uncertainties in both mechanical and electrical subsystems. A full state feedback mechanism is adopted under the assumption that joint positions, velocities, and phase currents are all measurable and available for control.

The joint position tracking objective is mathematically formulated by defining the tracking error signal $e(t) \in \mathbb{R}^n$ as

$$e \triangleq q_d - q, \quad (6)$$

where $q_d(t) \in \mathbb{R}^n$ denotes the desired trajectory, along with its first three time derivatives, is assumed to be bounded to allow practical controller design. An auxiliary error like term $r(t) \in \mathbb{R}^n$ is given by the equation

$$r \triangleq \dot{e} + K_ee, \quad (7)$$

where $K_e \in \mathbb{R}^{n\times n}$ refers to the control gain matrix, which is both diagonal and positive definite. By differentiating equation (7) with respect to time, pre-multiplying by $M(q)$, and utilizing the dynamics from (1), we derive the following compact representation for the open loop error dynamics

$$M\dot{r} = S - V_mr - K_{T1}I_BI_a - K_{T2}I_a, \quad (8)$$

where $S(q, q_d, \dot{q}, \dot{q}_d, \ddot{q}_d) \in \mathbb{R}^n$ contains modeling uncertainties and can be expressed as

$$S \triangleq M(q)\left(\ddot{q}_d + K_e\dot{e}\right) + V_m\left(q,\dot{q}\right)\left(\dot{q}_d + K_ee\right) + G(q) + F_d\dot{q}. \quad (9)$$

The dynamics of $I_a$ can be obtained via utilizing the backstepping procedure; therefore, to facilitate backstepping control, we define $\eta_a(t) \in \mathbb{R}^n$ as

$$\eta_a \triangleq I_{ac} - I_a, \quad (10)$$

where $I_{ac}(t) \in \mathbb{R}^n$ acts as a virtual control law within the structure of the backstepping approach. Inserting (10) into (8), yields the updated form of the equation

$$M\dot{r} = \tilde{S} + S_d - V_mr - K_{T1}I_BI_a + K_{T2}\eta_a - K_{T2}I_{ac}, \quad (11)$$

where $\tilde{S}(t) \triangleq S - S_d \in \mathbb{R}^n$, and $S_d\left(q_d, \dot{q}_d, \ddot{q}_d\right) \in \mathbb{R}^n$ is obtained via $S_d(t) \triangleq S|_{q=q_d,\dot{q}=\dot{q}_d}$. The norm of $\tilde{S}$ can be upper bounded as given below

$$\left\|\tilde{S}\right\| \le \left(\phi_1 + \phi_2\left\|e\right\|\right)\left\|e\right\| + \left(\phi_3 + \phi_4\left\|e\right\|\right)\left\|r\right\| \quad (12)$$

where $\phi_1$, $\phi_2$, $\phi_3$, and $\phi_4 \in \mathbb{R}$ define positive bounding constants.

*Property 3:* By leveraging the universal approximation property of orthogonal basis functions, the term $S_d$ can be expressed as

$$S_d \triangleq \varphi_dp_d + \epsilon_d, \quad (13)$$

where $\varphi_d(t) \in \mathbb{R}^{n\times n_d}$ denotes the Legendre polynomial-based orthogonal basis function matrix, with $n_d = n_{p_d} \cdot n_{s_d}$, in which $n_{p_d} \in \mathbb{R}$ denotes the degree of Legendre

polynomial, while $n_{s_d} \in \mathbb{R}$ corresponds to the number of evenly spaced sample points within the interval $[-1, +1]$, $\epsilon_d(t) \in \mathbb{R}^n$ is the truncation error introduced by the finite-term approximation, and $p_d \in \mathbb{R}^{n_d}$ represents the vector of unknown Legendre coefficients. For further details on the universal approximation property of orthogonal basis functions, refer to [19].

Based on open loop error dynamics provided in (11), along with the derived stability conditions, the virtual controller $I_{ac}(t)$ is formulated as follows

$$I_{ac} = \bar{K}_{T2}^{-1}\left(K_r r + (k_{a1} + k_{a2})\|e\|^2 r + e + \varphi_d \hat{p}_d\right), \quad (14)$$

where $\bar{K}_{T2} \in \mathbb{R}^{n\times n}$ defines the nominal value of the uncertain torque transmission matrix $K_{T2}$, $K_r \in \mathbb{R}^{n\times n}$ is represented as a diagonal matrix with strictly positive entries, serving as the control gain., $k_{a1}, k_{a2} \in \mathbb{R}$ are positive control gains, and $\hat{p}_d \in \mathbb{R}^{n_d}$ represents the estimate of unknown Legendre coefficients vector which is updated according to

$$\dot{\hat{p}}_d \triangleq \Gamma_d \varphi_d^T r, \quad (15)$$

where $\Gamma_d \in \mathbb{R}^{n_d \times n_d}$ denotes a diagonal and symmetric matrix with positive definiteness, used as the adaptation gain.

By inserting equations (13) and (14) into (11), the closed loop error dynamics of $r(t)$ can be reached as follows

$$\begin{aligned} M\dot{r} \;=\; & \tilde{S} - \varphi_d \tilde{p}_d + \epsilon_d - V_m r - K_{T1} I_B I_a + \bar{K}_{T2}\eta_a \\ & + \tilde{K}_{T2} I_a - K_r r - (k_{a1} + k_{a2})\|e\|^2 r - e, \end{aligned} \quad (16)$$

where $\tilde{p}_d(t) \triangleq \hat{p}_d - p_d \in \mathbb{R}^{n_d}$ defines the estimation error of the Legendre coefficients, and $\tilde{K}_{T2} \triangleq \bar{K}_{T2} - K_{T2} \in \mathbb{R}^{n\times n}$ represents the discrepancy between the actual and nominal values of the unknown torque transmission constant $K_{T2}$. The inequality $\left\|\tilde{K}_{T2} I_a\right\| \leq \rho \|\eta_a\|$ holds, with $\rho(t) \in \mathbb{R}$ representing a time–varying positive bound.

The dynamics of $\eta_a$ can be derived by taking the time derivative of (10), pre-multiplying the resulting expression by $L_a$, and substituting the electrical dynamics from (2) into the resulting expression, to yield

$$L_a \dot{\eta}_a = S_e - V_a, \quad (17)$$

where $S_e(t) \in \mathbb{R}^n$ represents the lumped uncertainty in electrical dynamics and is defined as

$$S_e \triangleq L_a \frac{dI_{ac}}{dt} + RI_a + N_p L_b I_B \dot{q} + K_{T2}\dot{q}. \quad (18)$$

Utilizing the universal approximation property of orthogonal basis functions as stated in Property 3, the term $S_e$ can be rewritten as follows

$$S_e \triangleq \varphi_e p_e + \epsilon_e, \quad (19)$$

where $\varphi_e(t) \in \mathbb{R}^{n\times n_e}$ is the Legendre polynomial-based orthogonal basis function matrix, with $n_e = n_{p_e} \cdot n_{s_e}$, in which $n_{p_e} \in \mathbb{R}$ denotes the degree of Legendre polynomial and $n_{s_e} \in \mathbb{R}$ is the number of evenly spaced sample points within the interval $[-1, +1]$, $\epsilon_e(t) \in \mathbb{R}^n$ contains the truncation error introduced by the finite-term approximation, and $p_e \in \mathbb{R}^{n_e}$ denotes the vector of unknown Legendre coefficients. The adaptation law for the estimate of $p_e$, shown with $\hat{p}_e \in \mathbb{R}^{n_e}$ is designed as

$$\dot{\hat{p}}_e \triangleq \Gamma_e \varphi_e^T \eta_a, \quad (20)$$

where $\Gamma_e \in \mathbb{R}^{n_e \times n_e}$ represents a diagonal and symmetric matrix with positive definiteness, used as the adaptation gain.

The phase voltage $V_a$ (*i.e.*, control input) is designed as follows

$$V_a = \varphi_e \hat{p}_e + K_a \eta_a + \bar{K}_{T2} r + k_n \rho^2 \eta_a, \quad (21)$$

where $K_a \in \mathbb{R}^{n\times n}$ defines a positive definite, diagonal gain matrix, while $k_n \in \mathbb{R}$ denotes a scalar control gain. Inserting (19) and (21) into (17), the closed loop dynamics of $\eta_a(t)$ yields the following

$$L_a \dot{\eta}_a = -\varphi_e \tilde{p}_e + \epsilon_a - K_a \eta_a - \bar{K}_{T2} r - k_n \rho^2 \eta_a \quad (22)$$

where $\tilde{p}_e(t) \triangleq \hat{p}_e - p_e \in \mathbb{R}^{n_e}$ defines the estimation error of the Legendre coefficients.

The open loop dynamics of $I_b$ can be given by the following expression

$$L_b \frac{dI_b}{dt} = S_b \theta_b + V_b + K_{T1} I_A r, \quad (23)$$

where $S_b(I_a, I_b, \dot{q}, r) \in \mathbb{R}^{n\times n_b}$ represents known regressor matrix, and $\theta_b \in \mathbb{R}^{n_b}$ defines unknown parameter vector, both of which are obtained from

$$S_b \theta_b \triangleq -RI_b + N_p L_a I_A \dot{q} - K_{T1} I_A r. \quad (24)$$

The phase voltage $V_b$ (*i.e.*, control input) is designed as

$$V_b \triangleq -S_b \hat{\theta}_b - K_b I_b, \quad (25)$$

where $\hat{\theta}_b(t) \in \mathbb{R}^{n_b}$ is the estimation of the uncertain parameter vector $\theta_b$ that is updated according to

$$\dot{\hat{\theta}}_b = \Gamma_b S_b^T I_b, \quad (26)$$

where $\Gamma_b \in \mathbb{R}^{n_b \times n_b}$ is defined as a diagonal adaptation gain matrix that is symmetric and positive definite. It should be noted that to ensure the boundedness of parameter estimations a projection operator can be used [21]. By applying equations (24) and (25) to (23), we can reach the closed loop dynamics of $I_b$ as follows

$$L_b \frac{dI_b}{dt} = -S_b \tilde{\theta}_b - K_b I_b + K_{T1} I_A r \quad (27)$$

where $\tilde{\theta}_b(t) \triangleq \hat{\theta}_b - \theta_b \in \mathbb{R}^{n_b}$ defines the parameter estimation error. We now proceed with the stability analysis.

## IV. Stability Analysis

*Theorem 1:* The phase voltages designed in (21), (25), and the adaptation laws designed in (15), (20), and (26) ensure that all signals remain bounded during closed loop operation and establish the semi-global uniform ultimate boundedness

[22] of the tracking error, assuming the controller gains are selected to satisfy the following conditions

$$\lambda_{\min}(K_e) > \kappa_e + \frac{1}{4\delta} + \frac{\phi_2^2}{4k_{a1}} \tag{28}$$

$$\lambda_{\min}(K_r) > \kappa_r + \frac{1}{4k_n} + \delta\phi_1^2 + \phi_3 + \frac{\phi_4}{4k_{a2}} + \delta_d \tag{29}$$

$$\lambda_{\min}(K_a) > \kappa_a + \delta_e \tag{30}$$

where $\kappa_e$, $\kappa_r$, $\kappa_a \in \mathbb{R}$ represent positive control gains, $\delta$, $\delta_d$, $\delta_e \in \mathbb{R}$ are positive damping constants.

*Proof:* As part of the proof for Theorem 1, a non-negative function $V(e, r, \eta_a, I_b, \tilde{p}_d, \tilde{p}_e, \tilde{\theta}_b) \in \mathbb{R}$ is introduced with the following structure

$$\begin{aligned} V \triangleq\ & \frac{1}{2}e^T e + \frac{1}{2}r^T M r + \frac{1}{2}\eta_a^T L_a \eta_a + \frac{1}{2}I_b^T L_b I_b \\ & + \frac{1}{2}\tilde{p}_d^T \Gamma_d^{-1} \tilde{p}_d + \frac{1}{2}\tilde{p}_e^T \Gamma_e^{-1} \tilde{p}_e + \frac{1}{2}\tilde{\theta}_b^T \Gamma_b^{-1} \tilde{\theta}_b. \end{aligned} \tag{31}$$

The expression in (31) can be upper and lower bounded as

$$\gamma_1 \|s\|^2 \leq V \leq \gamma_2 \|s\|^2 + \xi, \tag{32}$$

where $s(t) \triangleq [e^T, r^T, \eta_a^T, I_b^T]^T \in \mathbb{R}^{4n}$ is the combined error vector, and $\gamma_1$, $\gamma_2 \in \mathbb{R}$ are used to represent positive bounding constants defined as

$$\gamma_1 \triangleq \frac{1}{2}\min\{1, m_1, \lambda_{\min}(L_a), \lambda_{\min}(L_b)\}, \tag{33}$$

$$\gamma_2 \triangleq \frac{1}{2}\max\{1, m_2, \lambda_{\max}(L_a), \lambda_{\max}(L_b)\}, \tag{34}$$

$$\begin{aligned} \xi \triangleq\ & \frac{1}{2}\lambda_{\max}(\Gamma_d^{-1})\bar{\tilde{p}}_d^2 + \frac{1}{2}\lambda_{\max}(\Gamma_e^{-1})\bar{\tilde{p}}_e^2 \\ & + \frac{1}{2}\lambda_{\max}(\Gamma_b^{-1})\bar{\tilde{\theta}}_b^2, \end{aligned} \tag{35}$$

in which $\bar{\tilde{p}}_d$, $\bar{\tilde{p}}_e$, $\bar{\tilde{\theta}}_b \in \mathbb{R}$ denote positive constants that satisfy $\|\tilde{p}_d\| \leq \bar{\tilde{p}}_d$, $\|\tilde{p}_e\| \leq \bar{\tilde{p}}_e$, and $\left\|\tilde{\theta}_b\right\| \leq \bar{\tilde{\theta}}_b$, and $\lambda_{\min}(\cdot)$, $\lambda_{\max}(\cdot)$ denote the smallest and biggest eigenvalues of a square matrix, respectively.

After substituting the definition in (7) for $\dot{e}$, the closed-loop dynamics in (16), (22), (27), and (15), (20), (26) into the time derivative of (31), we obtain

$$\begin{aligned} \dot{V} =\ & -e^T K_e e + r^T \tilde{S} + r^T \tilde{K}_{T2} I_a - r^T \varphi_d \tilde{p}_d + r^T \epsilon_d \\ & - r^T K_r r - (k_{a1} + k_{a2}) \|e\|^2 \|r\|^2 - \eta_a^T \varphi_e \tilde{p}_e \\ & + \eta_a^T \epsilon_e - \eta_a^T K_a \eta_a - \eta_a^T k_n \rho^2 \eta_a - I_b^T S_b \tilde{\theta}_b \\ & - I_b^T K_b I_b + \tilde{p}_d^T \varphi_d^T r + \tilde{p}_e^T \varphi_e^T \eta_a + \tilde{\theta}_b^T S_b^T I_b. \end{aligned} \tag{36}$$

By reorganizing the terms and applying the square completion method, along with the upper bound on $\left\|\tilde{S}\right\|$ provided in (12), we obtain the following upper bound for the right hand side of (36) as

$$\begin{aligned} \dot{V} \leq\ & -\left(\lambda_{\min}(K_e) - \frac{1}{4\delta} - \frac{\phi_2^2}{4k_{a1}}\right)\|e\|^2 \\ & - \left(\lambda_{\min}(K_r) - \frac{1}{4k_n} - \delta\phi_1^2 - \phi_3 \right. \\ & \left. - \frac{\phi_4}{4k_{a2}} - \delta_d\right)\|r\|^2 - (\lambda_{\min}(K_a) - \delta_e)\|\eta_a\|^2 \\ & - \lambda_{\min}(K_b)\|I_b\|^2 + \frac{\bar{\epsilon}_d^2}{4\delta_d} + \frac{\bar{\epsilon}_e^2}{4\delta_e}, \end{aligned} \tag{37}$$

where Young's inequality [23] is applied in the following forms: $\|r\|\left\|\tilde{S}\right\| - (k_{a1} + k_{a2})\|e\|^2\|r\|^2 \leq \delta\phi_1^2\|r\|^2 + \frac{\phi_2^2}{4k_{a1}}\|e\|^2 + \phi_3\|r\|^2 + \frac{\phi_4^2}{4k_{a2}}\|r\|^2 + \frac{1}{4\delta}\|e\|^2$, $r^T\epsilon_d \leq \|r\|\bar{\epsilon}_d \leq \frac{\bar{\epsilon}_d^2}{4\delta_d} + \delta_d\|r\|^2$, $-r^T\left\|\tilde{K}_{T2}I_a\right\| - k_n\rho^2\|\eta_a\|^2 \leq \rho\|\eta_a\|\|r\| - k_n\rho^2\|\eta_a\|^2 \leq \frac{1}{4k_n}\|r\|^2$, and $\eta_a^T\epsilon_e \leq \|\eta_a\|\bar{\epsilon}_e \leq \frac{\bar{\epsilon}_e^2}{4\delta_e} + \delta_e\|\eta_a\|^2$. By utilizing the gain conditions in (28), (29), and (30), we can obtain further upper-bound for the right-hand side of (37) as follows

$$\dot{V} \leq -\gamma_3\|s\|^2 + \epsilon, \tag{38}$$

where $\gamma_3, \epsilon \in \mathbb{R}$ denote positive constants are defined as

$$\gamma_3 \triangleq \min\{\kappa_e, \kappa_r, \kappa_a, \lambda_{\min}(K_b)\}, \tag{39}$$

$$\epsilon \triangleq \frac{\bar{\epsilon}_d^2}{4\delta_d} + \frac{\bar{\epsilon}_e^2}{4\delta_e}. \tag{40}$$

The closed-loop signal boundedness is confirmed through standard signal analysis based on the results in (31) and (38). Moreover, the solution to the differential inequality obtained after substituting (32) into (38), leads to the conclusion that the tracking error satisfies semi-global uniform ultimate boundedness. ■

## V. Experimental Results

Experimental tests were carried out on a two dof robotic manipulator developed in a laboratory setting, as illustrated in Figure 1. To actuate the joints of the manipulator, Hobbywing-X8 type BLDC motors were employed, selected for their suitability in position-based motion control applications due to their torque speed characteristics. The rotational motion of the motors is transmitted to the robot joints via a planetary gearbox with an $8:1$ reduction ratio. High-resolution magnetic encoders (AS5047) are utilized to measure the angular motion of each joint. Furthermore, the mathematical model of the BLDC motors incorporates the Park/Clarke transformations, as described in (2) and (3). To accurately capture the motor dynamics, the inverse Park/Clarke transformation of phase currents and the forward transformation of applied voltages must be executed at high frequencies. To achieve this, each motor is equipped with a dedicated local driver (STM32F303RE and IHM-08M1), while the main control algorithm is executed on a host computer via an NI PCIe-6351 data acquisition card. The control loop and data communication between the host computer and the local motor drivers are maintained at a

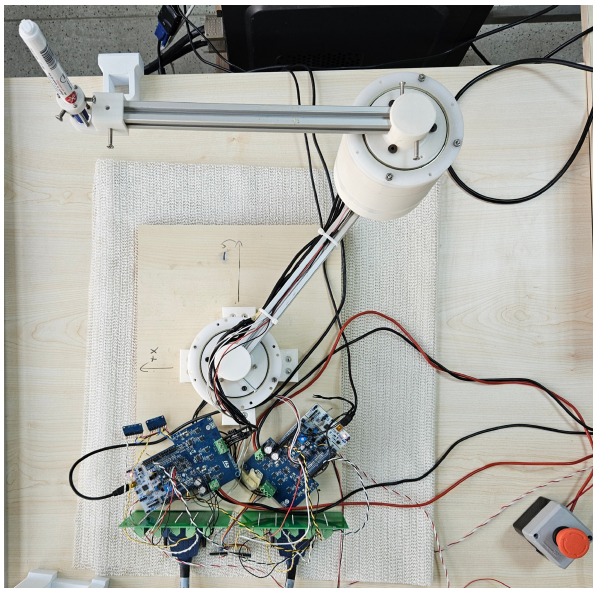

Fig. 1. Experimental setup: 2 dof robotic arm actuated by BLDC motors.

frequency of 1 kHz, while the local drivers function at 16 kHz.

At the start of the experiment, the manipulator was positioned at rest with initial joint positions $q(0) = [0, 0]^T$ [rad], and the desired trajectory was defined as follows

$$q_d(t) = 0.1 + \begin{bmatrix} \frac{\pi}{4}\left(1 - \exp\{-0.01t^3\}\right)\sin(0.3t) \\ \frac{\pi}{4}\left(-1 + \exp\{-0.01t^3\}\right)\cos(0.3t) \end{bmatrix} [rad]. \tag{41}$$

Control parameters were set to the following values $K_r = \text{diag}\{35, 34\}$, $K_e = \text{diag}\{17, 15\}$, $K_a = \text{diag}\{2.1, 2\}$, $K_b = \text{diag}\{0.4, 0.4\}$, $k_{a1} + k_{a2} = 15$, $k_n = 1$, $\rho = 0.3$, $\Gamma_d = 0.5$, $\Gamma_e = 0.2$, and $\Gamma_b = \text{diag}\{0.9, 0.09, 0.9, 0.09\}$. The degrees of Legendre polynomials were truncated at $n_{p_d} = n_{p_e} = 5$, with $n_{s_d} = n_{s_e} = 100$ number of evenly spaced sample points within the interval $[-1, +1]$. For adaptive parameter estimation $n_b = 4$. The nominal value of the unknown torque transmission constant was specified as $\bar{K}_{T2} = \text{diag}\{2.5, 2.2\}$.

A detailed presentation of the experimental outcomes is provided in Figures 2-5. The joint position tracking error $e(t)$ is shown in Figure 2 while in Figure 3, the actual joint positions and the desired trajectories are demonstrated. From Figures 2 and 3, it can be seen that the actual joint trajectories closely follow the desired trajectories as the tracking errors for both joints converge to a small neighborhood of zero. Figures 4 and 5 illustrate the control inputs $V_a$ and $V_b$ for both joints. The obtained practical results highlight the performance of the proposed controller in achieving precise tracking for robotic manipulators driven by BLDC motors.

## VI. Conclusions

This study presented a novel control framework that leveraged the orthogonality of Legendre polynomials to address mechanical-electrical uncertainties in BLDC-actuated robot arms. By explicitly incorporating actuator dynamics and employing the backstepping approach, the proposed controller effectively managed the coupled and nonlinear dynamics of such systems. Unlike many existing studies that relied on direct torque control and often neglected actuator dynamics, our approach provided a more comprehensive solution. Rigorous Lyapunov-based stability analysis confirmed the semi-global uniform ultimate boundedness of the closed-loop system, while experimental validation on a two dof robotic manipulator, developed in a laboratory setting, demonstrated low joint-space position tracking errors and practical feasibility.

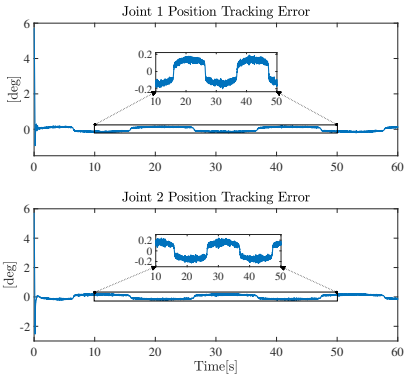


Fig. 2. Joint space tracking error $e(t)$

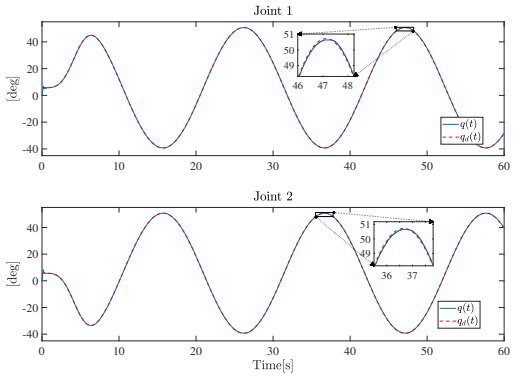


Fig. 3. Joint positions vs. desired trajectories

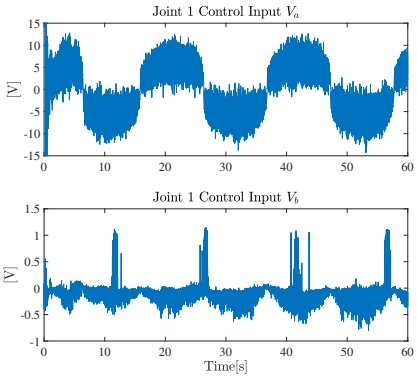


Fig. 4. Control voltages for the first joint

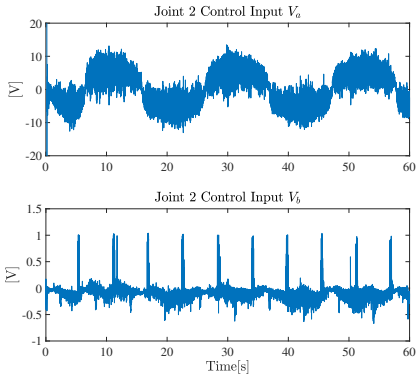


Fig. 5. Control voltages for the second joint

A key distinction of our work is its adaptation of advanced control techniques specifically for BLDC-driven manipulators, significantly broadening its applicability. The use of orthogonal functions for uncertainty compensation not only capitalizes on their universal approximation capabilities but also simplifies the implementation of the control law. Unlike regressor-based approaches, which require the calculation of a system-specific regressor matrix, our method eliminates this cumbersome requirement. Additionally, compared to neural network-based controllers that involve tuning a large number of parameters, our design is computationally efficient and straightforward to implement. Furthermore, unlike fuzzy logic based control structures that rely on expert knowledge, our approach does not require such prior information, making it more convenient and generalizable. In conclusion, this work provides a solid foundation for future developments in the control of advanced robotic systems, offering both theoretical insights and practical benefits.

Future research will focus on extending this framework to more complex robotic systems, such as redundant manipulators, and integrating adaptive and learning-based techniques to enhance performance under time-varying uncertainties and external disturbances. These advancements are expected to yield even more resilient and versatile control solutions, paving the way for practical applications across diverse robotic platforms.

## ACKNOWLEDGMENT

This study was supported by the Scientific and Technological Research Council of Türkiye (TUBITAK) under Grant Number 124E563 & 2219 Postdoctoral programs. The authors thank TUBITAK for their support.

## REFERENCES

[1] M. R. Diprasetya, S. Yuwono, M. Löppenberg, and A. Schwung, "Integration of ABB robot manipulators and robot operating system for industrial automation," in *International Conference on Industrial Informatics*, pp. 1–7, 2023.

[2] I. Tamadon, S. M. H. Sadati, V. Mamone, V. Ferrari, C. Bergeles, and A. Menciassi, "Semiautonomous robotic manipulator for minimally invasive aortic valve replacement," *IEEE Transactions on Robotics*, vol. 39, no. 6, pp. 4500–4519, 2023.

[3] M. Vikhe, N. Bothra, N. Malaviya, M. Kothari, and R. Koshti, "Four legged parallel manipulator for autonomous delivery robot," in *International Conference on Device Intelligence, Computing and Communication Technologies*, pp. 346–350, 2023.

[4] D. Mohanraj, R. Aruldavid, R. Verma, K. Sathiyasekar, A. B. Barnawi, B. Chokkalingam, and L. Mihet-Popa, "A review of BLDC motor: State of art, advanced control techniques, and applications," *IEEE Access*, vol. 10, pp. 54833–54869, 2022.

[5] P. I.-T. Chang, X.-Y. Lin, and I.-J. Yu, "Sensorless BLDC motor sliding mode controller design for interference recovery," in *International Conference on Control, Decision and Information Technologies (CoDIT)*, pp. 1780–1785, 2019.

[6] C. M. Verrelli, "Adaptive learning control design for robotic manipulators driven by permanent magnet synchronous motors," *International Journal of Control*, vol. 84, no. 6, pp. 1024–1030, 2011.

[7] D. Ebeigbe, T. Nguyen, H. Richter, and D. Simon, "Robust regressor-free control of rigid robots using function approximations," *IEEE Transactions on Control Systems Technology*, vol. 28, no. 4, pp. 1433–1446, 2019.

[8] C. K. Paul, B. Shankar Dey, and I. N. Kar, "Safe human robot-interaction using switched model reference admittance control," in *International Conference on Control, Decision and Information Technologies (CoDIT)*, pp. 1589–1594, 2024.

[9] B. M. Yilmaz, E. Tatlicioglu, A. Savran, and M. Alci, "Robust state/output-feedback control of robotic manipulators: An adaptive fuzzy-logic-based approach with self-organized membership functions," *IEEE Transactions on Systems, Man, and Cybernetics: Systems*, vol. 53, no. 5, pp. 3219–3229, 2023.

[10] M. R. Soltanpour, J. Khalilpour, and M. Soltani, "Robust nonlinear control of robot manipulator with uncertainties in kinematics, dynamics and actuator models," *International Journal of Innovative Computing, Information and Control*, vol. 8, no. 8, pp. 5487–5498, 2012.

[11] J. Moreno-Valenzuela, R. Campa, and V. Santibáñez, "Model-based control of a class of voltage-driven robot manipulators with non-passive dynamics," *Computers & Electrical Engineering*, vol. 39, no. 7, pp. 2086–2099, 2013.

[12] I. Saka, S. Unver, E. Selim, E. Tatlicioglu, and E. Zergeroglu, "Robust backstepping control of robotic manipulators actuated via brushless DC motors," *International Journal of Dynamics and Control*, vol. 12, no. 11, pp. 4110–4119, 2024.

[13] V. M. Hernández-Guzmán and J. Orrante-Sakanassi, "PID control of robot manipulators actuated by BLDC motors," *International Journal of Control*, vol. 94, no. 2, pp. 267–276, 2021.

[14] I. Saka, S. Unver, E. Selim, E. Zergeroglu, and E. Tatlicioglu, "An experimentally verified robust backstepping approach for controlling robotic manipulators actuated via brushless DC motors," *Control Engineering Practice*, vol. 153, p. 106073, 2024.

[15] Ş. Ünver, E. Selim, E. Tatlicioglu, E. Zergeroglu, and M. Alcı, "Adaptive control of BLDC driven robot manipulators in task space," *IET Control Theory & Applications*, vol. 18, p. 1910–1921, 2024.

[16] A. Izadbakhsh and S. Khorashadizadeh, "Robust adaptive control of robot manipulators using Bernstein polynomials as universal approximator," *International Journal of Robust and Nonlinear Control*, vol. 30, no. 7, pp. 2719–2735, 2020.

[17] M. Bajodek, F. Gouaisbaut, and A. Seuret, "Necessary and sufficient stability condition for time-delay systems arising from Legendre approximation," *IEEE Transactions on Automatic Control*, vol. 68, no. 10, pp. 6262–6269, 2023.

[18] A. Izadbakhsh, A. Deylami, and S. Khorashadizadeh, "Superiority of q-chlodowsky operators versus fuzzy systems and neural networks: Application to adaptive impedance control of electrical manipulators," *Expert Systems with Applications*, vol. 209, p. 118249, 2022.

[19] S. Khorashadizadeh, M. M. Zirkohi, H. Eliasi, and R. Gholipour, "Adaptive control of robot manipulators driven by permanent magnet synchronous motors using orthogonal functions theorem," *Journal of Vibration and Control*, vol. 29, no. 11-12, pp. 2789–2801, 2023.

[20] F. L. Lewis, D. M. Dawson, and C. T. Abdallah, *Robot manipulator control: Theory and practice*. CRC Press, 2003.

[21] D. Braganza, W. Dixon, D. Dawson, and B. Xian, "Tracking control for robot manipulators with kinematic and dynamic uncertainty," in *IEEE Conference on Decision and Control*, pp. 5293–5297, 2005.

[22] H. K. Khalil, *Nonlinear Systems.* Prentice-Hall, 2002.

[23] H. J. Marquez, *Nonlinear control systems: Analysis and design*. John Wiley & Sons, Inc., 2003.